The characterisation of aquifers by means of resistivity investigations

A. Bratus[1] and G. Santarato[2]

[1] *Istituto Nazionale di Oceanografia e Geofisica Sperimentale, Trieste, Italy*
[2] *Dipartimento di Scienze della Terra, Ferrara, Italy*

(Received: August 12, 2007; accepted: October 02, 2007)

ABSTRACT The present paper contains the description of a collection of data and the main results that were achieved in the frame of the CAMI project using resistivity-based methods. In particular, the Electrical Resistivity Tomography was used to get detailed 2D and 3D resistivity models of the shallowest part of the subsurface in the test area (down to some tens of metres), while to reach the whole designed investigation depth, Magnetotellurics and Time-Domain ElectroMagnetic method (TDEM) were used and their costs-to-benefits ratios were evaluated. As far as the results of the resistivity investigation are concerned, a reliable 4D model of the resistivity distribution down to more than 500 m b.g.l. was obtained by TDEM data inversion. This model showed the variations of the resistivity vs. time of the first confined aquifer which were in excellent agreement with direct data. A reliable estimation of the actual porosity was also obtained for the same aquifer.

1. Introduction

Geophysical methods that estimate electrical resistivity are widely used for mapping as well as for the characterization of aquifers. In fact, electrical resistivity is strictly related to water content and to its quality in terms of TDS (Total Dissolved Salts) through the well-known Archie's law (Archie, 1942), provided a porous, clay-free formation saturated with water is involved.

Geophysicists have developed several resistivity-based methods for exploration, characterization and quality monitoring of groundwater resources. All these methods share the same conceptual principle: a suitable source drives an electrical current into the subsurface, that in turn produces an artificial field whose characteristics are the function of the medium's resistivity distribution and the geometry of the field layout of the selected method. The physical quantities, measured on the Earth's surface, allow the so-called apparent resistivity to be determined. Suitable numerical inversion procedures permit us to estimate the true resistivity distribution.

The resistivity-based methods yield low spatial resolution models of the subsurface with respect to other geophysical methods such as reflection seismics; nevertheless, using proper geometrical and physical constraints, based on calibration data, a reliable estimate of the aquifer's resistivity can be achieved both in space and time, i.e. 3D and 4D models can be constructed.

Among these methods, perhaps the most studied and widely-used is the geo-electrical method, due to its simplicity both for data acquisition and in the processing stage. In this method, a direct current is injected into the subsurface by means of a couple of metallic electrodes, the electric

field generated is measured in between another couple of electrodes. Progress in micro-electronics has led to the development of the tomographic modality of resistivity data acquisition [i.e. Electrical Resistivity Tomography: ERT; Barker (1981)] accompanied by powerful 2D and 3D inversion schemes (e.g. Loke and Barker, 1996a, 1996b).

Unfortunately, the employment of this method for the exploration of depths beyond 100 m is hampered since the required separation of the quadripoles becomes impractical. In such cases, more sophisticated methods, based on the use of electromagnetic (EM) fields, are to be addressed.

In the Torrate (Friuli-Venezia Giulia, northeastern Italy) test site (Fig. 1), the characterization of the multi-aquifer system, hosted in the alluvial plain, was required. Based on previously available geophysical and hydrogeological reconnaissance studies (e.g. Giustiniani, 2005) the thickness of the fresh-water bearing sediments was postulated to be several hundred meters deep, so the authors decided to associate the EM method to the most appropriate methods capable of reaching great depths. Among the latter methods, the Magnetotelluric [MT, see e.g. Vozoff (1986)] and the Time-Domain Electromagnetic Method [TDEM, see e.g. McNeill (1994)] were selected, for the sake of assessing their costs-to-benefits ratio.

The main outcome of the integrated application of the above-mentioned geophysical methods, in terms of 4D characterization of alluvial aquifers, is described and critically discussed in this paper.

No outline of the subsurface geology and hydrogeology of the test area is reported here, since this information is extensively described in the paper of Rapti-Caputo and Vaccaro (2009).

2. Outline of the survey methods

As mentioned above, in the ERT method many electrodes are placed on the ground at even spacing, along one or more parallel profiles. All electrodes are connected to a multi-electrode geo-resistivity-meter which automatically spans all possible combinations of quadripoles. The array layout generally belongs to one of the well-known 4-electrode array layouts: Wenner (α), Schlumberger, dipole-dipole, pole-dipole and pole-pole, etc. The selection of the most suitable array depends on the specific properties of each array and the resistivity distribution of the medium.

In the MT method, temporal variations of the natural magnetic field act as the source of the current, which in turn induces a variable electric field in the subsurface. The investigation depth is controlled mainly by the selected frequency band for the operation, in agreement with the well-known "skin effect" of the EM fields. The "apparent resistivity" is determined by calculating the ratio of one horizontal component of the electric field (E_x, E_y) and the orthogonal horizontal component of the inducing magnetic field (H_x, H_y), at each frequency of the selected band.

In the TDEM method, a generally squared-shape loop of insulated and conducting wire is laid on the terrain, and a pulsed current is fed into it. Once the current is switched off, the rapid variation of the magnetic flux induces, in the subsurface, a current loop that mimics the transmitting loop, like a "smoke ring". The current ring propagates downwards, with a rate that depends on the resistivity of the encountered layers, and is progressively absorbed on account of the Joule effect. The associated magnetic field induces a transient electromotive force (e.m.f.) in the receiving coil, whose intensity decreases at the same rate as the current ring fades downwards.

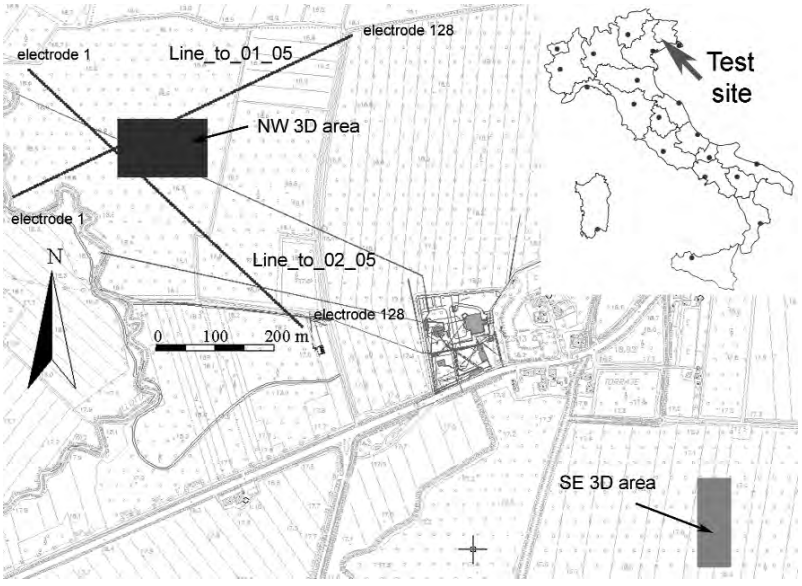

Fig. 1 - Location of the ERT measurements. ERT1, ERT2. 2D profiles, ERT 3D NW, ERT 3D SE: areas of 3D investigations.

Therefore, an apparent resistivity can be defined, which depends on that of the e.m.f. and time lapse after cut-off.

In all the above-described methods the physical property determined in the field is the apparent resistivity.

To estimate the true resistivity distribution within the investigated subsurface an inversion procedure is needed, which minimizes the difference between the experimental, apparent resistivities and the calculated ones based upon a "trial" model of the true resistivity distribution, under the same field data collection conditions. Unfortunately, inversion of the apparent resistivity data collected by the above methods is strongly non linear and the problem is "ill-posed". To overcome these problems, the inversion is performed using a suitable regularization procedure (Tikhonov and Arsenin, 1977). The most common inversion scheme is the so-called "Occam's inversion" (Constable *et al.*, 1987), where the requested minimization is reached using the minimum "roughness" of the model as the stabilizing function and a minimum information initial model represented by a homogeneous half-space.

3. Data acquisition

In the Torrate area, both 2D and 3D ERT data acquisition schemes were used, as shown in Fig. 1. Two 2D profiles were located in the NW part of the test area. Each profile was acquired with 128 electrodes at a 5 m spacing, resulting in a total length of 635 m. The Wenner array was employed to collect good quality, apparent resistivity data as well as to favour the inference of the horizontal discontinuities. In fact, like in previously collected data (Giustiniani *et al.*, 2009), the subsurface geology can be considered 1D at least from the geometrical point of view.

Two zones located in the NW and in the SE parts of the test site were chosen to undertake a

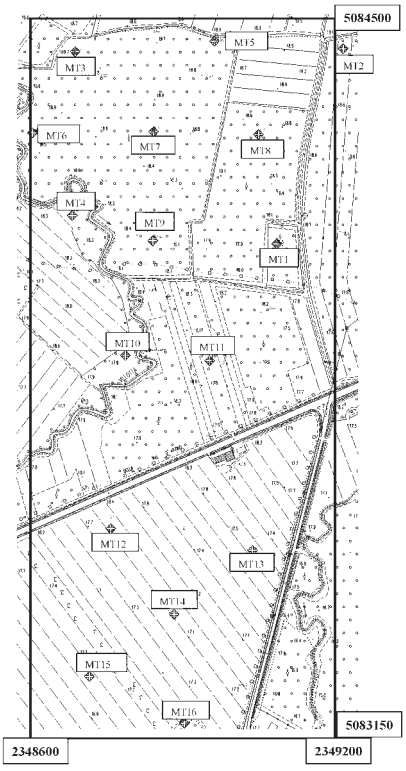

Fig. 2 - MT sounding locations (October 2005 survey).

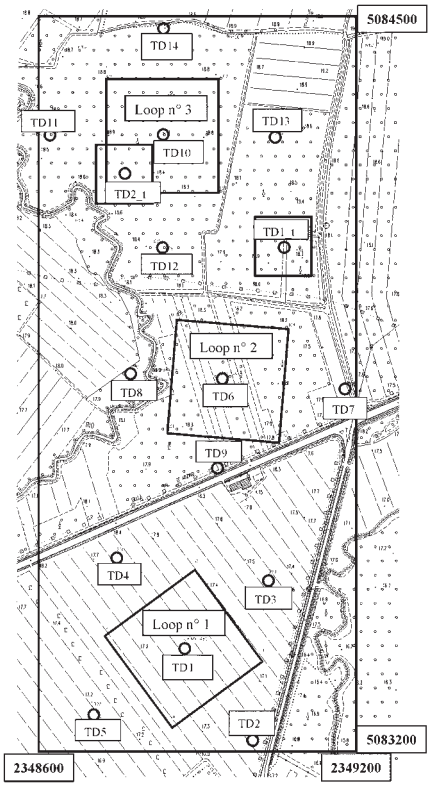

Fig. 3 - TDEM: soundings location (October 2005 survey)

3D ERT survey. In this case, 16 profiles, composed of 64 electrodes at 5 m intervals, were laid on the terrain. The dipole-dipole array was chosen to collect the data, in order to get the maximum lateral resolution. These 3D surveys were, in fact, aimed mainly at getting detailed information of the overburdened sediments to assess the vulnerability against contamination of the first confined aquifer.

MT data were acquired in October 2005, in 16 homogeneously distributed sounding points (Fig. 2). Stratagem equipment was used to collect the data in the frequency band between 10 Hz and 90 kHz. This band was considered sufficient to reach the desired depth of investigation. Analysis of the collected time series of the horizontal EM field components were Fourier's transformed and, subsequently, the apparent resistivity curves were calculated on site using the code embedded in the field equipment and afterwards in the lab using Chave's algorithm (Chave and Thomson, 1989).

TDEM data were acquired in two phases: the first, acquired simultaneously with the MT survey, where the sounding points were almost coincident (Fig. 3); the second, acquired in April 2006, where the southernmost loop of the former phase was moved towards the NE part of the test site (Fig. 4). This decision was based on the results of the previous TDEM survey, which showed the wedging of the first confined aquifer southwards. Nevertheless, data acquisition parameters were the same (i.e.

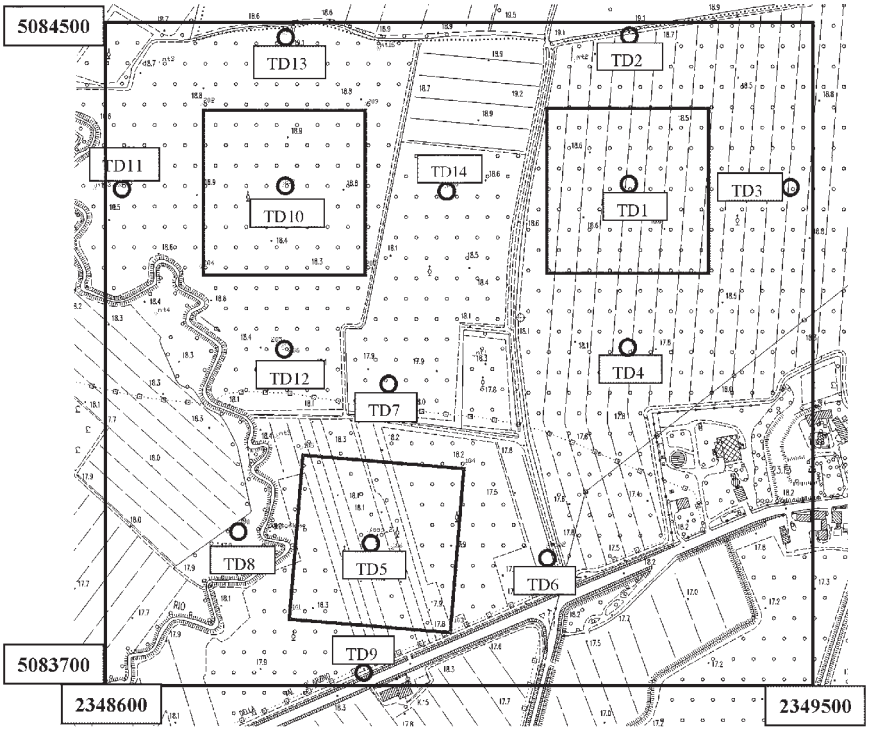

Fig. 4 - TDEM: soundings locations (April 2006 survey).

the three transmitter loops were squares of 200 m a side lengths and receiver coil 100 loops of 1 m^2). A total of sixteen central and out-of-loop soundings were carried out. Their locations were carefully selected in both surveys so as to result in an almost regular grid of 200 m spacing.

The dates were chosen with the aim of comparing the resistivity responses of the aquifers in two different phases of their exploitation: at the end of the summer season, when the water request is highest, and in spring, when aquifers are recharged.

4. Results

4.1. ERT survey

The ERT survey furnished detailed information about the shallowest subsurface to a depth of 100 m.

In order to optimise the data acquisition phase, a realistic 2D model of the subsurface of the area was devised (Fig. 5, top), based upon the available litho-stratigraphic data of boreholes distributed in the area. The geological sections were forward modelled to calculate the resistivity response using a free 2D modelling code. Model parameters are reported in Table 1.

Layer 1 was simulated as lens-shaped to reflect the lithology changes of the overburdened sediments and to evaluate possible effects of these changes on the apparent resistivity pseudo-section and on the inverted field model. The apparent resistivities thus obtained were inverted using the RES2DINV package (Loke and Barker, 1996a, 1996b). The results of the inversion of

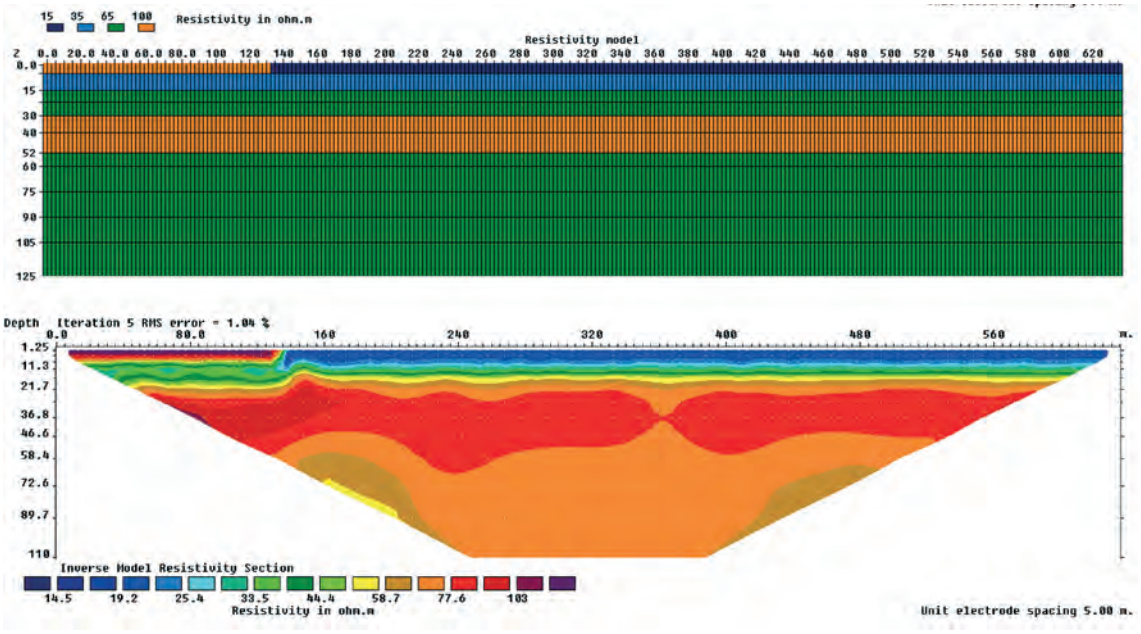

Fig. 5 - Top: the synthetic model of the 2D resistivity profile; bottom: the inverted resistivity model of the synthetic data.

the forward data are shown in the lower part of Fig. 5. As can be seen, the shallow discontinuity perturbs, to some extent, the reconstruction of the underlying layers. As a consequence, the image of the aquifer A1 (see Table 1) does not seem continuous.

The apparent field resistivity data were collected using the same parameters employed in the forward modelling (Fig. 6). Good quality apparent resistivity data for both profiles became a low RMS error of 2.1% and 1.29% at the end of the iterative inversion process.

In the resistivity models, the resistivity values around 14.5 Ωm, shown in blue, correspond to the clay level, while resistivity values around 90 Ωm (red colour) are associated to the porous sandy level, i.e. the A1 aquifer. Green (resistivity values around 40 Ωm) corresponds to a clay-silt level. Therefore, the heteropy of the overburden is satisfactorily resolved, but, as shown above,

Table 1 - Parameters of the 2D forward resistivity model.

Layer No.	Lithology	Resistivity (Ω.m)	Depth (m)	Thickness (m)
1	Clay / Gravel	15 / 100	0	5
2	Silty Clay	35	5	10
3	Clayey silt	65	15	15
4	Sandy aquifer(A1)	100	30	22
5	Clayey silt	65	52	undefined

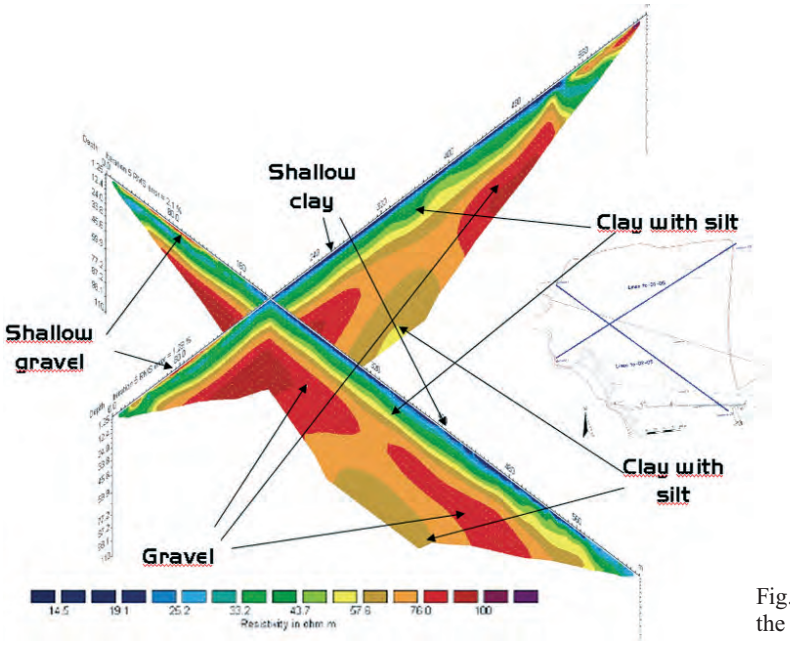

Fig. 6 - Fence resistivity diagram of the two 2D ERT models

its presence perturbs both the upper surface and the lateral continuity of the underlying formations; as a consequence, the aquifer body is laterally continuous without noteworthy heterogeneities. Furthermore, the bottom of the A1 aquifer is also identified, since resistivity decreases, below 55 m, to values that can be attributed to the presence of an impermeable clay horizon that constitutes the aquiclude of the first confined hydrogeological unit.

The inversion of the 3D data was performed along the acquisition profiles, using the same 2D inversion software. The 3D volume distribution of the resistivity data was achieved by geostatistical interpolation as the geometry of the subsurface was known to be simple. One example is shown in Fig. 7, where the gently undulating morphology of the top of the A1 aquifer is evident.

In Fig. 8, we show two 2D inversion profiles that concern the electrical stratigraphy of the two 3D areas: the first pertains to the NW 3D survey, and clearly shows marked lateral heterogeneity of the overburden sediments, while the second, pertaining to the SW 3D survey, indicates a different situation, i.e. the overburden is characterized by higher resistivity values indicating the presence of coarse-grained sediments. The situation at depth remains similar to that of the NW part. The clay level and the A1 aquifer can be recognized in both models.

4.2. MT survey

The apparent MT resistivities of all soundings turned out to be affected by an unfavourable signal-to-noise (S/N) ratio (Fig. 9), which is particularly strong for periods greater than 3.10^{-3} s as can be inferred by the anomalous slopes of both apparent rsistivity and phase curves. Consequently, a 1D joint inversion of apparent resistivity and phase data led to quite inconsistent model parameters for depths greater than 100 m, throughout all the soundings. The inconsistency

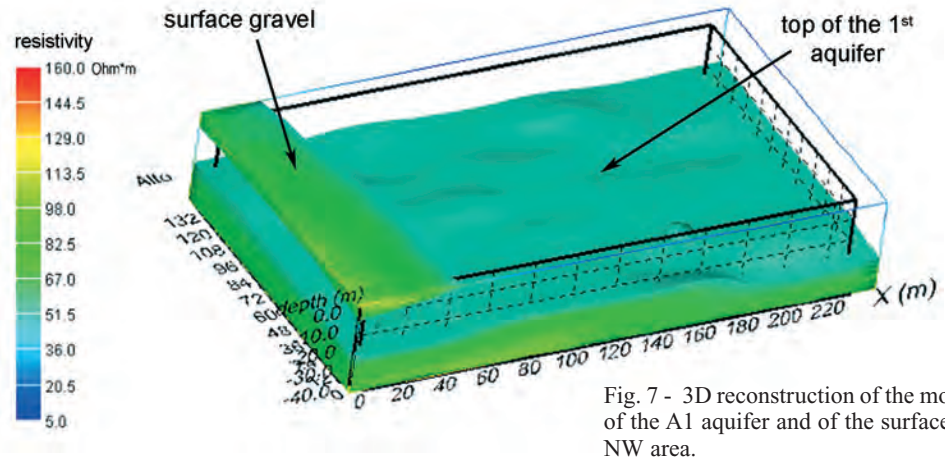

Fig. 7 - 3D reconstruction of the morphology of the top of the A1 aquifer and of the surface gravel layer of the NW area.

was supported by previous geometrical and geological knowledge at those depths. To get more reliable data, a wide-band artificial source should have been used; but this choice would have greatly complicated the data acquisition phase, given the relatively high resistivities present in the subsurface. For this reason, and considering the much more consistent TDEM resistivity inferred models at the desired depths, the April 2006 survey, planned to get 4D information, was carried out using only the TDEM method.

4.3. TDEM surveys

The first TDEM survey was carried out in October 2005 simultaneously with the MT survey, while the second was repeated in April 2006. The apparent resistivities obtained were inverted using Occam's 1D procedure (Constable *et al.*, 1987), without constraints. The 1D models obtained were geostatistically interpolated to produce a 3D resistivity model of the subsurface (Figs. 10 and 11).

First of all, we can observe that the TDEM soundings explored depths of no less than 500 m. At greater depths, the S/N ratio becomes too low to accurately resolve the bottom of the high resistivity layer centred at around a 450 m depth b.g.l..

Secondly, a resistive horizon, centred around 50 m b.g.l., was identified, which wedges southwards according to the results of the October 2005 first TDEM survey and becomes thicker passing from the October 2005 to the April 2006 TDEM survey. The meaning of this resistive horizon is quite clear: it coincides with the resistive body of the ERT results (Fig. 6) and represents the TDEM response of the A1 aquifer. The observed variation in time must be associated with the electrical conductivity (EC) variation of the fresh water since it can't be attributed to a change in the subsurface geology. In fact, hydrogeological data have confirmed this result: in October 2005, the A1 EC was about 530 µS/cm in the test area, while in May 2006, it decreased to 460 µS/cm. This decrease of water conductivity is strictly concurrent with the hydrogeological regime of this aquifer: highly exploited during the summer and recharged with low-conductivity rainwater in winter/spring.

The explanation for the observed deep high-resistivity horizon was fully understood after the

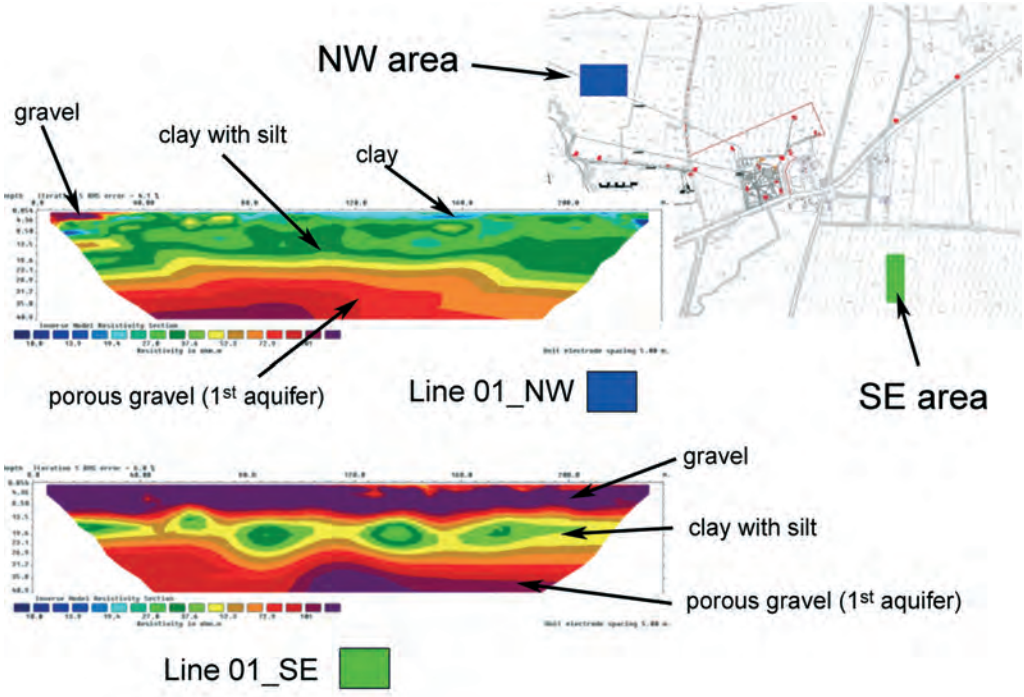

Fig. 8 - Examples of 2D resistivity models obtained in the two 3D acquisition areas.

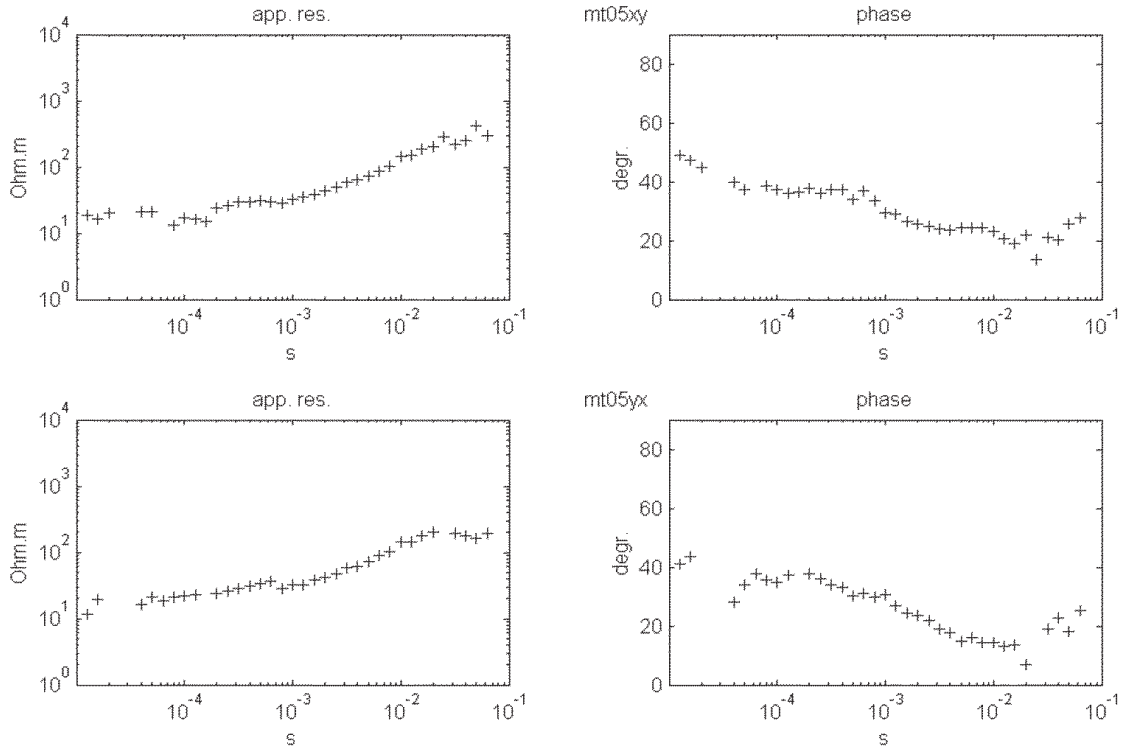

Fig. 9 - An example of MT data (sounding no. 5).

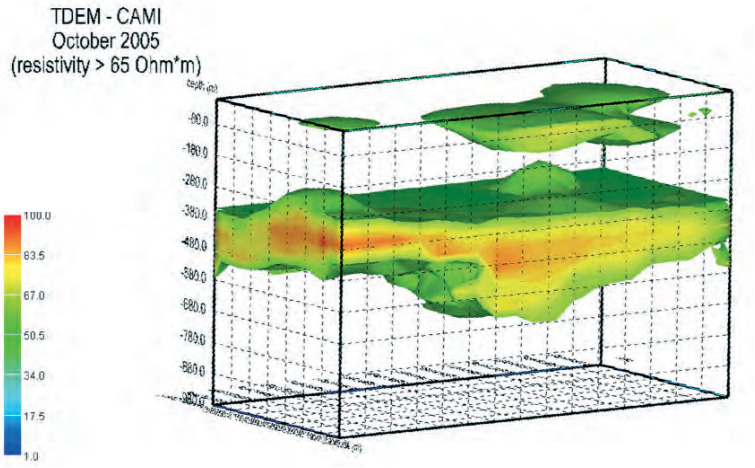

Fig. 10 - 3D model of TDEM estimated resistivities, October 2005 survey; view from SE.

drilling of an exploratory borehole, completed with several geophysical logs to better characterize the water-bearing horizons. The borehole lithology indicated a thick gravel aquifer whose top is located at about 480 m b.g.l. and whose resistivity was found to be higher than the overlying and underlying aquiclude layers that consist mainly of clay. Note that the resistivity maximum of the TDEM sounding models was observed to be around 480 m b.g.l. This interface is also characterized by a strong seismic reflectivity, which is the cause of the fair seismic reflection observed in the 2D and 3D seismic results (see Giustiniani *et al.*, 2009; Picotti *et al.*, 2009; Tinivella *et al.*, 2009). So, the methods employed show a high degree of agreement.

5. Discussion and conclusions

As mentioned above, the 2D and 3D seismic results provided information about the geometry of the subsurface by reliably identifying the presence of several horizons with high reflectivity. Consequently, all the gathered ERT and TDEM apparent resistivity data were once again inverted, using a constrained 1D inversion scheme based on the Marquardt-Levenberg's approach (Marquardt, 1963). The goal was to define a more accurate estimate of each aquifer's resistivity, so that a reliable estimate of their effective porosity could be achieved at each sounding point. This was possible by using the well-known Archie relation (Archie, 1942). From the 2D ERT profiles, two vertical electric soundings (VES: L1_315 and L2_315) with a maximum a-spacing of 210 m were derived, using apparent resistivities measured at the respective centres at symmetrically increasing a-spacing. The inverted curves provided information to a depth of about 100 m. The best fitting 1D models are reported in Table 2.

Similarly, three VESs were also selected from the 3D ERT data collected in the south-eastern part of the test site, reaching a maximum quadripole length of 100 (L3_100, L3_110 and L3_120). The inversion results are reported in Table 3. Due to the smaller layout, the VES collected in the south-eastern area cannot give any information about the layer underlying the first confined aquifer. Nevertheless, the latter soundings indicate the presence of a resistive, i.e. porous, overburden in this

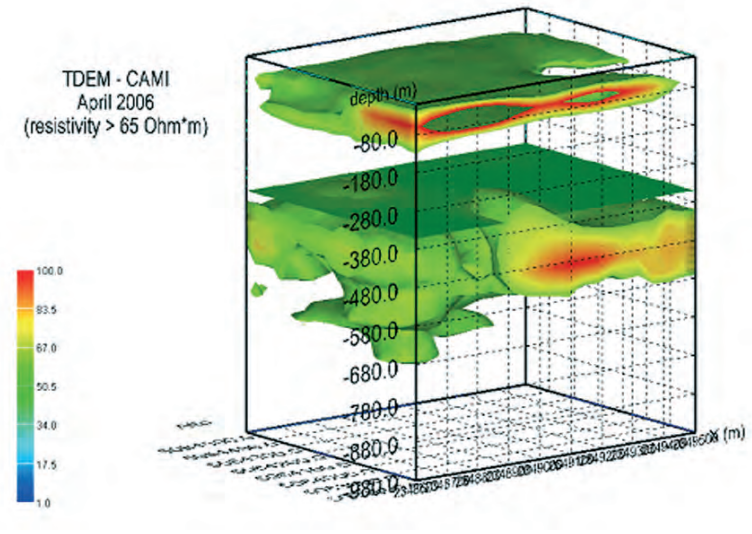

Fig. 11 - 3D model of TDEM estimated resistivities, April 2006 survey; view from SE.

part of the test area, while the first aquifer is protected by a relatively conductive, non-porous medium only 10 m thick.

As far as TDEM data are concerned, the 1D constrained inversion yielded the results reported in Table 4 (October 2005 survey) and Table 5 (April 2006 survey).

The sensitivity analysis of the TDEM data allowed us to resolve four layers above the substratum. The overburden has, in general, a low resistivity (20 to 30 Ωm); the second layer is characterized by resistivity values ranging between 43 and 80 Ωm, in the soundings pertaining to the southern loop of the October 2005 survey. Much higher resistivity values characterize this horizon in all the other soundings. A very thick and relatively good conducting layer separates layer no. 2 from layer no. 4 which is, in turn, quite resistive. In this layer, both resistivities and thicknesses of the best fitting models are quite variable, as occurs for the substratum resistivity. The reason for this lack of stability could be attributed to a poorer S/N ratio at the later time gates, when the investigation depths are greater than 500 m.

So, on the basis of indirect data, a reliable estimation of the effective porosity was possible using Archie's law (Archie, 1942) for a clay-free, saturated porous medium:

Table 2 - Parameters of the 1D constrained inversion models of the VESs extracted from the Wenner ERT profiles pertaining to the NW investigated area.

VES	Layer 1: resistivity	Layer 1: thickness	Layer 2: resistivity	Layer 2: thickness	Layer 3: resistivity
L1_315	31	27	117	28	66
L2_315	31	27	105	28	69

Table 3 - Parameters of the 1D constrained inversion models of the VESs extracted from three dipole-dipole ERT profiles pertaining to the SE investigated area.

VES	Layer 1: resistivity	Layer 1: thickness	Layer 2: resistivity	Layer 2: thickness	Layer 3: resistivity
L3_100	130	20	27	10	130
L3_110	150	19	24	10	130
L3_120	144	18	28	11	130

$$\rho = a\rho_w \Phi^m,$$

where ρ is the resistivity of the water-bearing medium, ρ_w is the water resistivity and Φ is its effective porosity. Choosing a =1 and the cementation factor m =1.3, for a loose sediment as suggested from the literature, (e.g., Schoen, 1996) an average porosity of 24% can be estimated for aquifer A1, which can be used to estimate the potential volume of water contained in it.

Now we are in a position to draw several concluding remarks:

1. there is a fair agreement between the resistivity estimates reported in Tables 2 and 4, especially for coincident sounding points, i.e. the centres of the two ERT profiles 1 and 2 and the TDEM soundings nos. 10 and 12, although the acquisition parameters for TDEM data collection were devised to get information from depths greater than 50 m b.g.l.;
2. since for fresh-water bearing sediments there is a relation between decreasing grain size and decreasing resistivity, due to increasing clay content, the southward decrease of resistivity values in the October's 2005 TDEM survey means that the first confined aquifer is not present there, since the sediment matrix becomes enriched with fine sediments;
3. as far as the TDEM soundings pertaining to the two surveys are concerned, the resistivities of layer no. 2 increase by an average factor of 13%: this increment is strictly linked to the observed decrease of the EC of the fresh water contained in the A1 aquifer, which corresponds to this layer;
4. layer no. 4 shows resistivity values that can easily be attributed, based on previously available geological information, to loose porous sediments, saturated with fresh water.

Finally, a part from the good agreement between the TDEM and ERT resistivity distribution estimates thanks to a satisfactory superposition at the common investigation depths, perhaps the most surprising result has been that the TDEM repeated surveys have recorded the EC variations of the water contained in the first confined aquifer precisely, thus in excellent agreement with the direct hydrogeological information.

All the above results confirm that the whole set of geoelectrical methods is a reliable, cost-effective tool for hydrogeological exploration and monitoring.

Acknowledgements. The activities described in the present paper are part of the CAMI project, funded by the EC contract LIFE04 ENV/IT/00500. The Authors warmly aknowledge dr. Daniel Nieto Yàbar for the effective and skilled scientific coordination of the CAMI project. Field assistance in the TDEM data

Table 4 - Parameters of the 1D constrained inversion models of the TDEM soundings pertaining to the October 2005 survey.

sounding	Layer 1: resistivity	Layer 1: thickness	Layer 2: resistivity	Layer 2: thickness	Layer 3: resistivity	Layer 3: thickness	Layer 4: resistivity	Layer 4: thickness	Layer 5: resistivity	Rms %
Td1_t	20	25	150	32	60	400	150	170	21	3.9
Td2_t	21	27	115	30	59	400	100	180	4	3.1
Td1	24	23	130	30	38	400	90	210	1	4.3
Td2	23	25	46	25	40	400	210	180	3.5	4
Td3	27	23	43	28	40	400	180	140	1	2.5
Td4	20	25	44	28	biased	by	passive	noise	source	
Td5	26	24	80	28	38	400	130	240	3	2.4
Td6	22	31	165	29	42	400	235	276	4	
Td7	17	27	104	33	47	390	125	180	11	2.6
Td8	23	29	118	32	38	400	140	215	7	1.3
Td9	biased	by	nearby	passive	noise	source				
Td10	18	26	122	37	52	400	33	113	10	3.4
Td11	22	28	84	27	52	400	68	60	12	1.9
Td12	19	27	105	30	54	400	80	130	9	4
Td13	20	29	120	27	56	400	70	130	18	2.1
Td14	18	24	120	28	55	410	82	120	13	1.7

Table 5 - Parameters of the 1D constrained inversion models of the TDEM soundings pertaining to the April 2006 survey.

Sounding	Layer 1: resistivity	Layer 1: thickness	Layer 2: resistivity	Layer 2: thickness	Layer 3: resistivity	Layer 3: thickness	Layer 4: resistivity	Layer 4: thickness	Layer 5: resistivity	Rms %
Td1	31	31	95	24	60	400	110	240	18	3.1
Td2	20	23	92	27	52	410	135	230	15	1.6
Td3	23	23	106	26	50	400	110	190	12	2.5
Td4	20	25	120	26	53	400	80	160	7	2.9
Td5	19	27	212	40	40	352	205	220	3.5	3.2
Td6	14	23	154	36	49	390	180	130	5	3
Td7	19	28	114	30	49	400	80	130	5	3
Td8	21	29	136	32	39	400	145	175	6	3.5
Td9	biased	by	nearby	passive	noise	source				
Td10	18	27	144	36	58	400	107	300	24	4.5
Td11	20	28	108	27	54	400	85	150	14	2.2
Td12	19	26	140	30	57	400	98			3
Td13	19	28	155	27	58	400	87	130	20	1.8
Td14	17	24	153	28	56	410	100	330	17	4

collection and elaboration by Nasser Abu-Zeid and Riccardo De Nardi is also acknowledged, and likewise Alan Chave, for having made his source code for robust processing of MT time series available to the whole scientific community. This paper was presented at the 18th Electro-Magnetic Induction Workshop (EMIW), held in El Vendrell (Spain) September 17-23, 2006.

REFERENCES

Archie G.; 1942: *The electrical resistivity log as an aid in determining some reservoir characteristics.* Transactions of AIME, **146**, 54-62.

Barker R.D.; 1981: *Offset system of electrical resistivity sounding and its use with a multicore cable.* Geophysical Prospecting, **29**, 128-143.

Chave A.D. and Thomson D.J.; 1989: *Some comments on magnetotelluric response function estimation.* Journal of Geophysical Research, **94**, 14215-14226.

Constable S.C., Parker R.L. and Constable C.G.; 1987: *Occam's inversion - A practical algorithm for generating smooth models from electromagnetic sounding data.* Geophysics, **52**, 289–300.

Giustiniani M.; 2005: *Metodologie sismiche per la caratterizzazione di strutture e individuazione di risorse nella Regione Friuli-Venezia Giulia.* Doctorate thesis, unpublished, Università of Trieste, Italy.

Giustiniani M., Accaino F., Del Negro E., Picotti S. and Tinivella U.; 2009: *Characterisation of shallow aquifers by 2D high-resolution seismic data analysis.* Boll. Geof. Teor. Appl., **50**, 29-38.

Loke M.H. and Barker R.D.; 1996a: *Rapid least-squares inversion of apparent resistivity pseudosections by a quasi-Newton method.* Geophysical Prospecting, **44**, 131-152.

Loke M.H. and Barker R.D.; 1996b: *Practical techniques for 3D resistivity surveys and data inversion.* Geophysical Prospecting, **44**, 499-524.

Marquardt D.; 1963: *An algorithm for least-squares estimation of nonlinear parameters.* SIAM Journal of Applied Mathematics, **11**, 431-441.

McNeill J.D.; 1994: *Principles and application of time domain electromagnetic techniques for resistivity sounding.* Technical note n° 27, Geonics Ltd., Canada. 15 pp.

Picotti S., Giustiniani M., Accaino F. and Tinivella U.; 2009: *Depth modelling and imaging of the 4D seismic survey of the Basso Livenza area (NE Italy).* Boll. Geof. Teor. Appl., **50**, 71-82.

Rapti-Caputo D. and Vaccaro C.; 2009: *Deep alluvial aquifer system: an example from the Tagliamento River hydrogeological basin (NE Italy).* Boll. Geof. Teor. Appl., **50,** 39-50.

Schoen J.H.; 1996: *Physical properties of rocks. Fundamentals and principles of Petrophysics.* Elsevier Science Ltd, Oxford (GB), 583 pp.

Tikhonov A.N. and Arsenin V.Y.; 1977: *Solutions of ill-posed problems.* Winston and Sons, Washington (DC), 272 pp.

Tinivella U., Accaino F., Giustiniani M. and Picotti S.; 2009: *Petro-physical characterization of shallow aquifers by using AVO and theoretical approaches.* Boll. Geof. Teor. Appl., **50**, 59-69.

Vozoff K.; 1986: *Magneto-telluric methods*. S.E.G. Geophysics Reprint Series No. 5, Society of Exploration Geophysicists, 766 pp.

Corresponding author: Giovanni Santarato
Universita' di Ferrara
Dipartimento di Scienze della Terra
via Saragat 1, 44100 Ferrara, Italy
phone: +39 0532 974728; fax: +39 0532 974767; e-mail: giovanni.santarato@unife.it